ISME

Dynamic Coupled Thermo-Viscoelasticity of a Spherical Hollow Domain

H. Eghbalian[*]
MSc.

M. R. Eslami[†]
Professor

The generalized coupled thermo-viscoelasticity of hollow sphere subjected to thermal symmetric shock load is presented in this paper. To overcome the infinite speed of thermal wave propagation, the Lord-Shulman theory is considered. Two coupled equations, namely, the radial equation of motion and the energy equation of a hollow sphere are obtained in dimensionless form. Resulting equations are transformed into the Laplace domain using the Laplace transformation and discretized by means of the finite element method along the radius. Week's method is employed to obtain the unknowns in the time domain. The numerical results are provided to examine the propagation of thermal and mechanical waves. The results presented visually as temporal, radial and stress-strain plots to shown wave front of various field variables.

Keywords: Thermo-viscoelasticity, Lord-Shulman model, Kelvin-Voigt model, Finite element model, Numerical Laplace inverse transformation.

1 Introduction

In the solid mechanics, the Fourier law of heat conduction is commonly used to describe the heat transfer phenomena. This model predicts the thermal wave propagation with infinite speed. Instead, the generalized thermoelasticity introduces the transmission of thermal wave with finite speed. There are several mathematical models which admit finite speed of thermal wave propagation and the second sound effects such as Lord-Shulman [1], Green-Lindsay [2], and Green-Naghdi [3, 4]. In the theory of Lord-Shulman, the Fourier law of heat conduction is adjusted by bringing the concept of relaxation time.

The theories of Green-Lindsay and Green-Naghdi pursue a more thermodynamical approach. Green and Lindsay offered two lag times in the stress-strain relation and entropy expression, based on works of Müller [5] and Green and Law [6]. Green and Naghdi introduced the concept of thermal displacement, and based on this concept they offer three distinct thermoelastic models which are known as type I, II, and III. The types II and III of Green-Naghdi theory demonstrate the second sound effect. The linearized form of type I is equivalent to the previous well-known Fourier law of heat conduction. The type II predicts a non-dissipative effect.

[*]MSc., Mechanical Engineering Department, South Tehran Branch, Islamic Azad University, Tehran, Iran eghbalian.hirad@gmail.com

[†]Corresponding Author, Professor, Mechanical Engineering Department, Amirkabir University of Technology, Tehran, Iran eslami@aut.ac.ir

However, the type III, which is combinatory form of types I and II, has a dissipative effect. Bagri and Eslami [7] suggested a unified model of thermoelasticity which contains all aforementioned models. Many researches have studied the contexts of generalized thermoelasticity [8-13].

Similar to the elastic materials, it is excepted to see the second sound effect in the viscoelastic materials. Ezzat et al. [14] formulated the generalized thermo-viscoelasticity using the state space approach. Othman et al. [15] proposed a solution for the two dimensional linear generalized thermo-viscoelasticity. El-Karamany and Ezzat [16] established a solution for the linear generalized thermo-viscoelasticity based on the Laplace transformation technique. Kar and Kanoria [17] studied the thermo-viscoelastic interaction on a homogeneous viscoelastic isotropic spherical shell in the context of generalized theories of thermo-elasticity.

In the present study, we present a dynamic coupled thermo-viscoelastic analysis for spherical hollow domains. The domain is considered to be subject of spherically symmetric heat shock, both in meridian and circumferential directions. The medium is made of homogenous and isotropic thermo-viscoelastic material. The Kelvin-Voigt rheological model in conjunction with conventional small deformation thermoelasticity is adjusted for explaining the thermo-viscoelastic behavior of the domain. The appropriate equation of motion and energy equation are derived in radial direction. The energy equation is derived based on the Lord-Shulman theory of generalized thermoelasticity. For the sake of numerical convenience, the governing equations are converted into a non-dimensional form. The weak form of non-dimensional governing equations are discretized using the one-dimensional trans-finite element method and results are obtained in the Laplace domain. In order to achieve the obtained variables in the time domain, a numerical Laplace inversion method must be considered. In this study, the Weeks method [18] is employed to obtain the unknowns in the real time domain. For validation consideration, the results are compared with the known data in literature.

The results are presented as distribution of stresses, displacement, and temperature with respect to the non-dimensional time and non-dimensional space variable in radial direction. Also, the stress-strain diagrams presented for different types of loading and the hysteresis effect are shown. Using the prepared finite element model, different numerical examples are solved. Consequently, effects of the viscous relaxation time and the rate of loading on the magnitude of stress wave fronts are obtained. In this way, the results reveal the effect of time dependent constitutive relation on the response of a spherical hollow domain to the different types of heat shock.

2 Preliminaries

2-1 Motion Equation

The equation of motion for the case of symmetric displacement in the spherical coordinates in absent of body force is

$$\frac{\partial \sigma_{rr}}{\partial r} + \frac{2\sigma_{rr} - \sigma_{\theta\theta} - \sigma_{\phi\phi}}{r} = \rho \ddot{u} \tag{1}$$

Where $(\dot{})$ indicates the derivative with respect to time. In above equation, σ_{rr}, $\sigma_{\theta\theta}$, and $\sigma_{\phi\phi}$ are the radial, meridian, and circumferential normal components of stress tensor, respectively. Also, the radial displacement is denoted by u and ρ is the mass density.

In order to model an isotropic homogeneous viscoelastic solid, Kelvin-Voigt is chosen. This model can be represented as shown in Figure (1) with help of spring and dashpot. Based on this model, the stress-strain relations are written as [19],

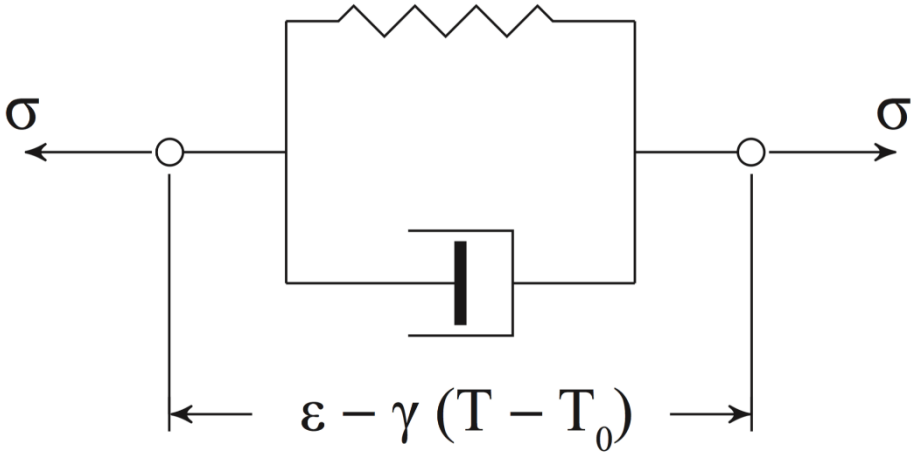

Figure 1 The intellectual diagram of Kelvin-Voigt thermo-viscoelastic model.

$$\sigma_{rr} = \left(1 + \tau\frac{\partial}{\partial t}\right)\left[2\mu\varepsilon_{rr} + \lambda\left(\varepsilon_{rr} + \varepsilon_{\theta\theta} + \varepsilon_{\phi\phi}\right) - \beta(T - T_0)\right]$$
$$\sigma_{\theta\theta} = \left(1 + \tau\frac{\partial}{\partial t}\right)\left[2\mu\varepsilon_{rr} + \lambda\left(\varepsilon_{rr} + \varepsilon_{\theta\theta} + \varepsilon_{\phi\phi}\right) - \beta(T - T_0)\right] \quad (2)$$
$$\sigma_{\phi\phi} = \left(1 + \tau\frac{\partial}{\partial t}\right)\left[2\mu\varepsilon_{rr} + \lambda\left(\varepsilon_{rr} + \varepsilon_{\theta\theta} + \varepsilon_{\phi\phi}\right) - \beta(T - T_0)\right]$$

Here, ε_{rr}, $\varepsilon_{\theta\theta}$, and $\varepsilon_{\phi\phi}$ are the strain tensor components, T and T_0 are the absolute and reference temperatures, λ and μ are the Lamé coefficients and β is the thermoelastic parameter which is defined as $\beta = (3\lambda + 2\mu)\gamma$, where γ is thermal expansion coefficient. In this model, it is assumed that the viscous effect acts on all components, including spherical and deviatoric, with similar viscous relaxation time of τ.

The components of strain tensor in spherical coordinates in terms of the displacement u and due to the meridian and circumferential symmetry are

$$\varepsilon_{rr} = \frac{\partial u}{\partial r}, \quad \varepsilon_{\theta\theta} = \varepsilon_{\phi\phi} = \frac{u}{r} \quad (3)$$

2-2 Energy Equation

The conventional Fourier law of heat conduction is modified as a result of the Lord-Shulman theory by introduction of a relaxation time t_0 in spherical coordinates as [1, 20]

$$\left(1 + t_0\frac{\partial}{\partial t}\right)q_r = -K\frac{\partial T}{\partial r} \quad (4)$$

Where q_r is the radial component of heat flux and K is the thermal conductivity coefficient. The linear form of the heat balance equation in term of radial heat flux q_r is obtained as [20],

$$\frac{1}{r^2}\frac{\partial(r^2 q_r)}{\partial r} + \beta T_0\left(\dot{\varepsilon}_{rr} + \dot{\varepsilon}_{\theta\theta} + \dot{\varepsilon}_{\phi\phi}\right) + \rho c\dot{T} = 0 \quad (5)$$

Here, c represents the specific heat at constant strain.

2-3 Equations in Non-Dimensional Form

Transferring the equations into the non-dimensional form is a practical approach in numerical computation physics. Using this method, numerical fluctuations and noises reduce and numerical stability increases in return. In order to do this, dimensionless variables are introduced as given below

$$r^* = \frac{r}{l}, \qquad (t^*.t_0^*.\tau^*) = \frac{(t.t_0.\tau)c_1}{l}, \qquad T = \frac{T - T_0}{T_d},$$
$$u^* = \frac{u(\lambda + 2\mu)}{l\beta T_d}, \quad (\sigma_{rr}.\sigma_{\theta\theta}.\sigma_{\phi\phi}) = \frac{(\sigma_{rr}.\sigma_{\theta\theta}.\sigma_{\phi\phi})}{\beta T_d}, \quad q_r^* = \frac{q_r l}{K T_d} \tag{6}$$

The symbol (*) indicates the dimensionless parameters. The parameter l is the characteristic length and is defined as $l = K(\rho c c_1)^{-1}$ and T_d is the designation temperature. Moreover, c_1 is the speed of propagation of primary elastic wave and is defined as $c_1 = \sqrt{(\lambda + 2\mu)/\rho}$. Considering the dimensionless parameters (6) and the governing Eqs. (1) and (5) and also the constitutive relations (2), (4), and strain-displacement relations (3), the non-dimensional form of these equations are obtained as

$$\frac{\partial \sigma_{rr}^*}{\partial r^*} + 2\frac{\sigma_{rr}^* - \sigma_{\theta\theta}^*}{r^*} = \frac{\partial^2 u^*}{\partial t^{*2}} \tag{7}$$

$$\frac{1}{r^{*2}}\frac{\partial (r^{*2} q_r^*)}{\partial r^*} + C_T \frac{\partial}{\partial t^*}\left(\frac{\partial u^*}{\partial r^*} + 2\frac{u^*}{r^*}\right) + \frac{\partial T^*}{\partial t^*} = 0 \tag{8}$$

$$\sigma_{rr}^* = \left(1 + \tau^* \frac{\partial}{\partial t^*}\right)\left[\frac{\partial u^*}{\partial r^*} + 2C_E \frac{u^*}{r^*} - T^*\right]$$
$$\sigma_{\theta\theta}^* = \left(1 + \tau^* \frac{\partial}{\partial t^*}\right)\left[C_E \frac{\partial u^*}{\partial r^*} + (1 + C_E)\frac{u^*}{r^*} - T^*\right] \tag{9}$$

$$\left(1 + t_0^* \frac{\partial}{\partial t^*}\right) q_r^* = -\frac{\partial T^*}{\partial r^*} \tag{10}$$

In Eqs. (8) and (9), C_E and C_T are coupling parameters corresponding to the elastic and thermoelastic effects, respectively. These coupling parameters are defined as

$$C_E = \frac{\lambda}{\lambda + 2\mu}, \quad C_T = \frac{\beta^2 T_0}{\rho c c_1^2} \tag{11}$$

3 Solution Method

3-1 Transfinite Element Formulation

The Galerkin method [21] is used to discretized the balance equations across the thickness of hollow sphere $\mathcal{B}$. Accordingly, the hollow sphere is divided into n_e concentric spherical elements $\mathcal{B}^{(e)}$ with equal thicknesses. Nodal values are considered on each sides of these spherical elements, as shown in Figure (1). These nodal values interpolate across the thickness of elements with the aid of appropriate shape functions.

$$\mathcal{B} = \bigcup_{e=1}^{n_e} \mathcal{B}^{(e)} \tag{12}$$

$$u^*(r^*.t^*)|_{\mathcal{B}^{(e)}} = \sum_{m=1}^{n_r} N_m(r^*)U_m^*(t^*)\,, \quad T^*(r^*.t^*)|_{\mathcal{B}^{(e)}} = \sum_{m=1}^{n_r} N_m(r^*)T_m^*(t^*) \tag{13}$$

where n_r is the number of nodal values across the thickness of $\mathcal{B}^{(e)}$, which is equal to two in this study. Here, N_m, U_m^*, and T_m^* are shape function and the nodal values of the radial displacement and temperature fields, respectively. The week from obtained by applying the Galerkin method to Eqs. (7) and (8) as following

$$\int_{\mathcal{B}} \left(\frac{\partial^2 u^*}{\partial t^{*2}} \delta u^* + \sigma_{rr}^* \frac{\partial \delta u^*}{\partial r^*} + 2\sigma_{\theta\theta}^* \frac{\delta u^*}{r^*} \right) dV^* = F_r^* \delta u^*|_{\partial\mathcal{B}} \tag{14}$$

$$\int_{\mathcal{B}} \left(q_r^* \frac{\partial \delta T^*}{\partial r^*} + C_T \frac{\partial}{\partial t^*} \left(\frac{\partial u^*}{\partial r^*} + 2\frac{u^*}{r^*} \right) \delta T^* + \frac{\partial T^*}{\partial t^*} \delta T^* \right) dV^* = -Q_r^* \delta u^*|_{\partial\mathcal{B}} \tag{15}$$

Here, F_r^* and $Q_r^*$are radial traction and heat flux over the surface of $\mathcal{B}$. Using Eqs (12) and (13) and substituting into Eqs. (14) and (15), also by aid of the Laplace transformation in case of vanished initial conditions, the transfinite element equations are obtained as

$$\begin{aligned} &\int_{\mathcal{B}^{(e)}} \Big[s^2 r^{*2} \{N\}\langle N\rangle + (1+\tau^* s)\Big(r^{*2} \Big\{\frac{\partial N}{\partial r^*}\Big\} \langle \frac{\partial N}{\partial r^*} \rangle \\ &\quad + 2r^* C_E \Big(\Big\{\frac{\partial N}{\partial r^*}\Big\} \langle N\rangle + \{N\} \langle \frac{\partial N}{\partial r^*} \rangle \Big) + 2(1+C_E)\{N\}\langle N\rangle \Big) \Big] dr^* \{\hat{U}^*\} \\ &- \int_{\mathcal{B}^{(e)}} \Big[(1+\tau^* s)\Big(r^{*2} \Big\{\frac{\partial N}{\partial r^*}\Big\} \langle N\rangle + 2r^* \{N\}\langle N\rangle \Big) \Big] dr^* \{\hat{T}^*\} = \frac{1}{4\pi} \hat{F}_r^* \{N\}\big|_{\partial\mathcal{B}^{(e)}} \end{aligned} \tag{16}$$

$$\begin{aligned} &\int_{\mathcal{B}^{(e)}} C_T s \Big[r^{*2} \{N\} \langle \frac{\partial N}{\partial r^*} \rangle + 2r^* \{N\}\langle N\rangle \Big] dr^* \{\hat{U}^*\} \\ &+ \int_{\mathcal{B}^{(e)}} \Big[\frac{r^{*2}}{1+t_0^* s} \Big\{\frac{\partial N}{\partial r^*}\Big\} \langle \frac{\partial N}{\partial r^*} \rangle + s r^* \{N\}\langle N\rangle \Big] dr^* \{\hat{T}^*\} = -\frac{1}{4\pi} \hat{Q}_r^* \{N\}\big|_{\partial\mathcal{B}^{(e)}} \end{aligned} \tag{17}$$

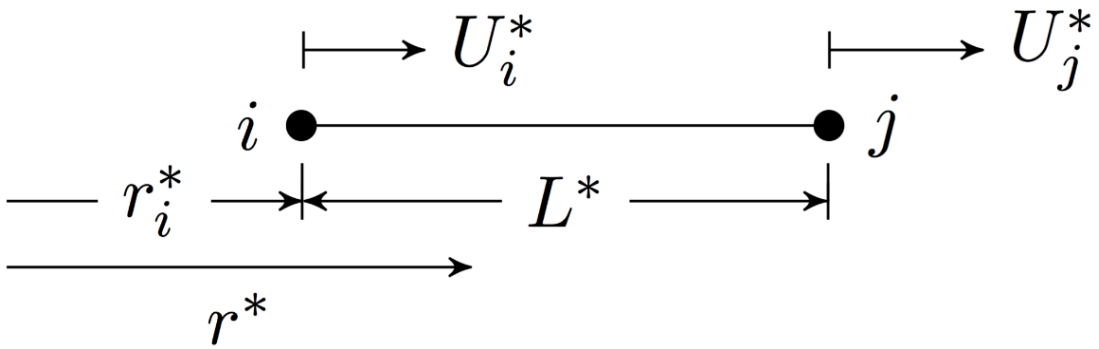

Figure 2 One dimensional simplex element along the thickness of hollow sphere.

In above equations, $(\widehat{\ })$ indicates the filed values in Laplace domain and s is the Laplace variable. Here, Eqs. (16) and (17) can be written in form of a linear system of algebraic equation in the Laplace domain after assembling all elements together.

$$\left[\hat{K}(s)\right]\left\{\hat{X}(s)\right\} = \left\{\hat{F}(s)\right\} \tag{18}$$

By solving Eq. (18), field variables are obtained in the Laplace domain. To transfer this field variables from the Laplace domain into the time domain, a numerical Laplace inversion method has been applied.

3-2 Numerical Laplace Inversion Method

In this study, the method of Weeks [18] is employed. This method is a series expansion method which uses the Laguerre orthonormal polynomials [22],

$$f(t) \cong e^{\sigma t}\sum_{j=0}^{\infty} a_j \mathrm{L}_j\left(\frac{t}{g}\right) \tag{19}$$

Where $L_j(\cdot)$ is the jth Laguerre polynomial and σ and g are scaling factors. Using M terms of approximation yields

$$\sigma = \Psi - \frac{1}{2g},\ \ T = 2g,\ \ g = \frac{t_{max}}{N},\ \ \Psi = \left(\alpha + \frac{1}{t_{max}}\right) H\left(\alpha + \frac{1}{t_{max}}\right) \tag{20}$$

Here, α is an optimizing parameter and $t_{\max}$ is the largest value of time needed to compute. In Eq. (20), $H(\cdot)$ is the unit step function. To calculate the value of weight parameters a_i in Eq. (19), following relations are used

$$\begin{aligned} a_0 &= \frac{1}{M+1}\sum_{k=0}^{M} h(\theta_k), \\ a_j &= \frac{2}{M+1}\sum_{k=0}^{M} h(\theta_k)\cos(2j\theta_k) \end{aligned} \tag{21}$$

which,

$$\theta_k = \frac{\pi}{2}\frac{2k+1}{M+1} \tag{22}$$

$$h(\theta) = \frac{M}{t_{\max}}\left\{Re\left[F\left(\Psi + \frac{i}{2g}\cot\frac{\theta_k}{2}\right)\right] - \cot\frac{\theta_k}{2}\, Im\left[F\left(\Psi + \frac{i}{2g}\cot\frac{\theta_k}{2}\right)\right]\right\}$$

4 Numerical Results and Discussion

A hollow sphere made of homogeneous isotropic material with dimensionless inside radii $r_i^* = 1$ and dimensionless outside radii $r_o^* = 2$ subjected to different cases of thermal loading is considered. The thermomechanical properties are considered as $\lambda = 40.4\ GPa$, $\mu = 27.0 GPa$, $\gamma = 23 \times 10^{-6}\ 1/K$, $\rho = 2707\ kg/m^3$, $K = 204\ W/m$, and $c = 903\ J/Kg\ K$.

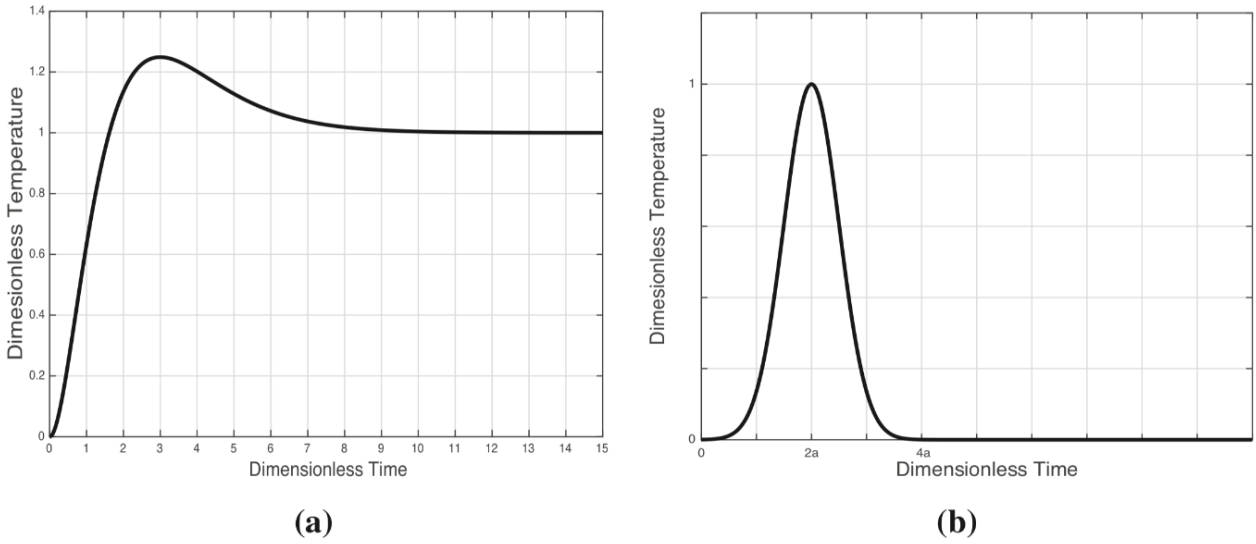

Figure 3 Thermal loading profiles, (a) the case I of thermal loading profile for validating results, (b) the case II of thermal loading profile in form of a thermal shock.

Eslami and Vahedi [20, 23, 24] solve the linear thermoelasticity of a hollow sphere using the finite element method. The results of this study are compared with those done by Eslami and Vahedi [20, 23, 24]. To compare the results, two cases of thermal loadings are presented, as given in Figure (3). The inside boundary of sphere is under thermal shock and the outside boundary is considered with zero displacement. As a result, the boundary conditions for these two cases of loadings are obtained as

$$T^*(r_i^*, t^*) = \begin{cases} 1 + \left(t^{*2} - t^* - 1\right)e^{-t^*} & case\ I \\ \exp\left(-\dfrac{(t^* - 4a)^2}{2a^2}\right) & case\ II \end{cases} \tag{23}$$

Also, the initial conditions are assumed to be zero across the thickness of sphere

$$u^*(r^*, 0) = \frac{\partial u^*}{\partial t^*}(r^*, 0) = T^*(r^*, 0) = 0 \tag{24}$$

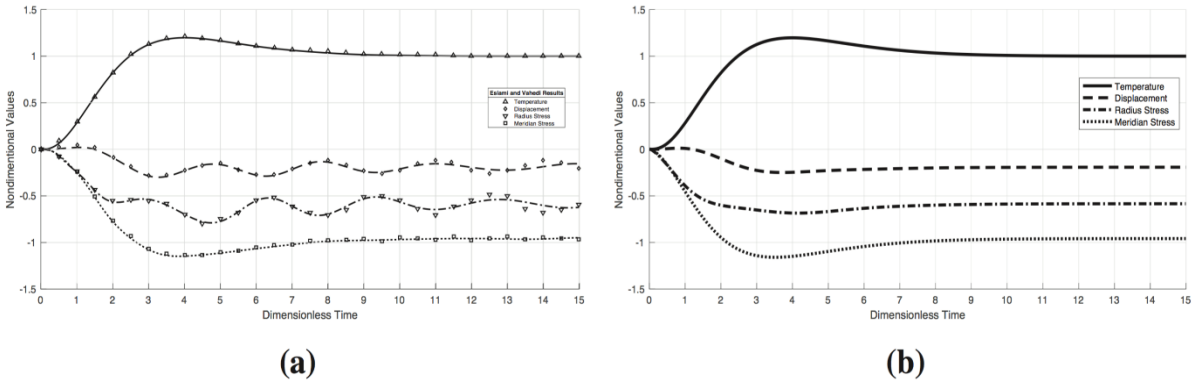

Figure 4 Variation of the non-dimensional field variables with respect to the dimensionless time at the middle point under the case I of thermal loading, (a) in absent of the thermal and viscoelastic relaxation effects and in comparison with Eslami and Vahedi results [20], and (b) with $\boldsymbol{\tau}^* = 0.4$ and no thermal relaxation effect.

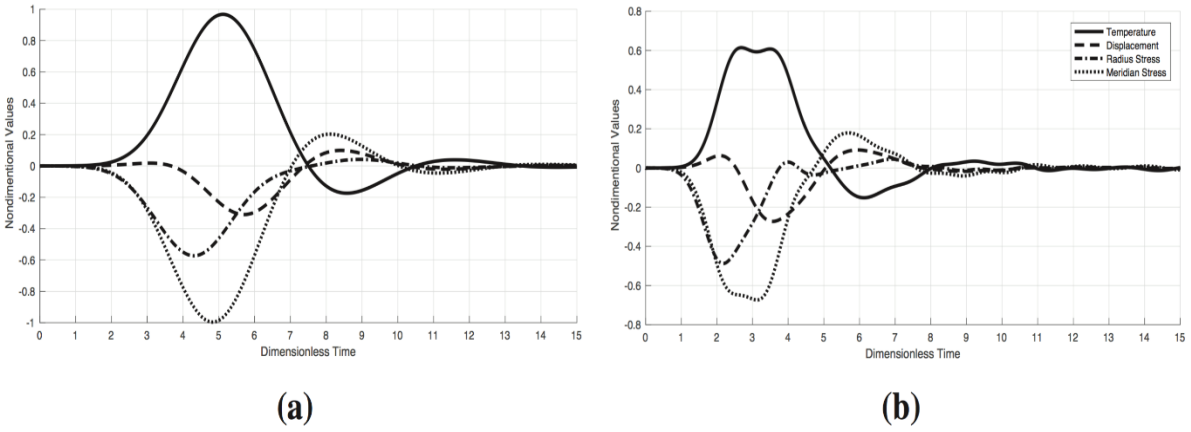

Figure 5 Variation of the non-dimensional field variables with respect to the dimensionless time at the middle point, considering thermal and viscous effects, under the case II of thermal loading with, (a) $\boldsymbol{a} = 1.0$, and (b) $\boldsymbol{a} = 0.5$.

4-1 Comparison Study

Considering a hollow sphere with the previous mentioned properties with the boundary and initial conditions of EQs. (23) and (24) under the case I of thermal loading in absent of all viscous and second sound effects. In this case, the temporal variation of dimensionless temperature, displacement, radial stress, and meridian stress are established as results of Figure (4a). These results are obtained by 100 elements and the Weeks parameters of $\alpha = 0.16$ and $M = 32$. By comparing these results with the previous results done by Eslami and Vahedi [20, 23, 24], an exceptional concurrence can be observed.

In the next step, the viscous relaxation time τ^* is considered as 0.4 and results are obtained. The non-dimensional field variables are obtained in Figure (4b). Clearly, it is seen that the wave fronts obtained in Figure (4a) are damped by the viscous effect in Figure (4b). It is, however, seen that the changes in temperature and meridian stress are not significant.

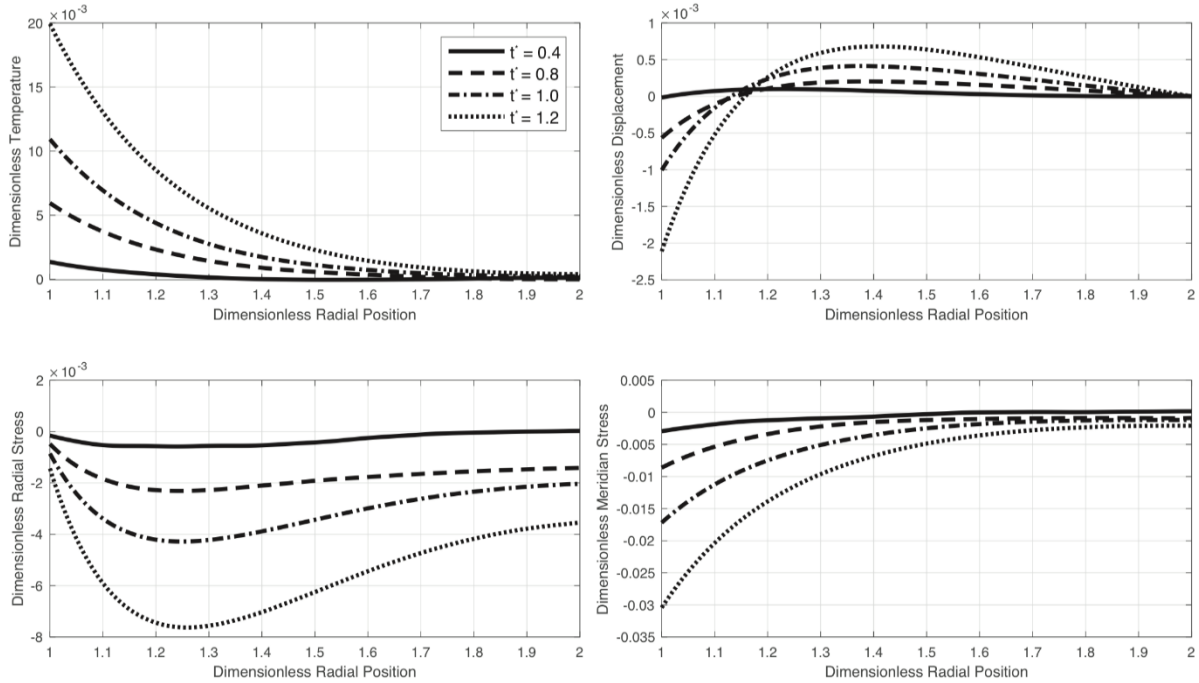

Figure 6 Variation of different dimensionless field variables with respect to the dimensionless radial position at various dimensionless times under the case II of thermal loading with $\boldsymbol{a} = 1.0$.

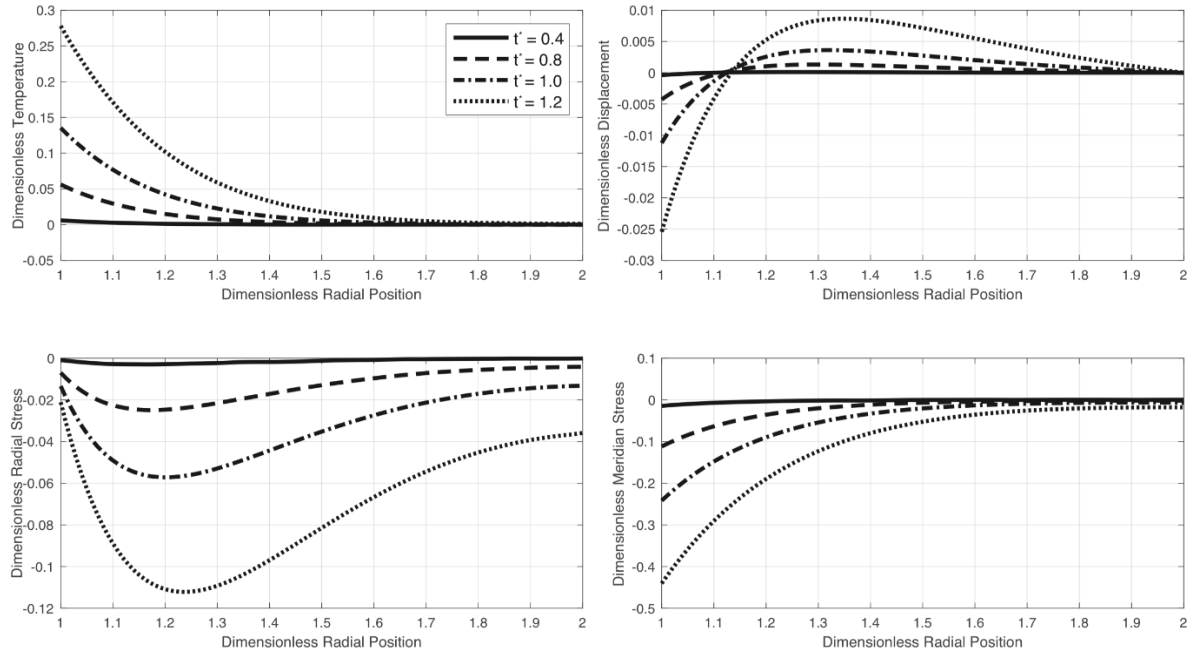

Figure 7 Variation of different dimensionless field variables with respect to the dimensionless radial position at various dimensionless times under the case II of thermal loading with $\boldsymbol{a} = 0.5$.

4-2 Thermal Shock Effects

A rapid temperature change is needed to reveal the second sound effect. Thus, the case II of thermal loading is applied with $a = 1.0$ and $a = 0.5$. In order to decrease numerical fluctuations, the Weeks parameter M is increased to 50. The results are obtained in Figures (5) to (7). The second sound effect is observed in Figure (5). Also, the influence of the thermal loading intensity is obvious.

Increasing the thermal loading intensity leads the results to have amplification in magnitude of field variables, as shown in Figures (6) and (7), because of rapid developing of thermal loading profile. However, the radial profile of field variables was not changed by increasing the thermal loading intensity in form-factor.

In Figure (8), the thermal and displacement wave fronts are visualized at three different points $Q1$, $Q2$, and $Q3$, which are placed in $r^* = 1.25$, $r^* = 1.5$, and $r^* = 1.75$, respectively. The waves motion show that the speed of propagation of the thermal wave is about two time faster that the speed of propagation of the displacement wave and they are in order of the speed of propagation of primary elastic wave of c_1.

4-3 Parametric Studies

In the last study, the influence of viscous relaxation time is studied. In Figure (9) the temporal variation of different non-dimensional field variables with respect to the distinct values of the viscous relaxation time are revealed. Figure (9) shows that the wave front of the displacement and stress fields are decreased by increasing the value of the viscous relaxation time. In other side, the peak values of the radial stress and meridian stress are increased due to the increasing of viscous relaxation time. Similar to the first study, the temperature field did not change significantly. In Figure (10) the loading paths are shown for $\tau^* = 0.5$ and $\tau^* = 2.0$. By increasing the value of viscous relaxation time, the surrounded area of stress-strain plane is increased by the hysteresis loop.

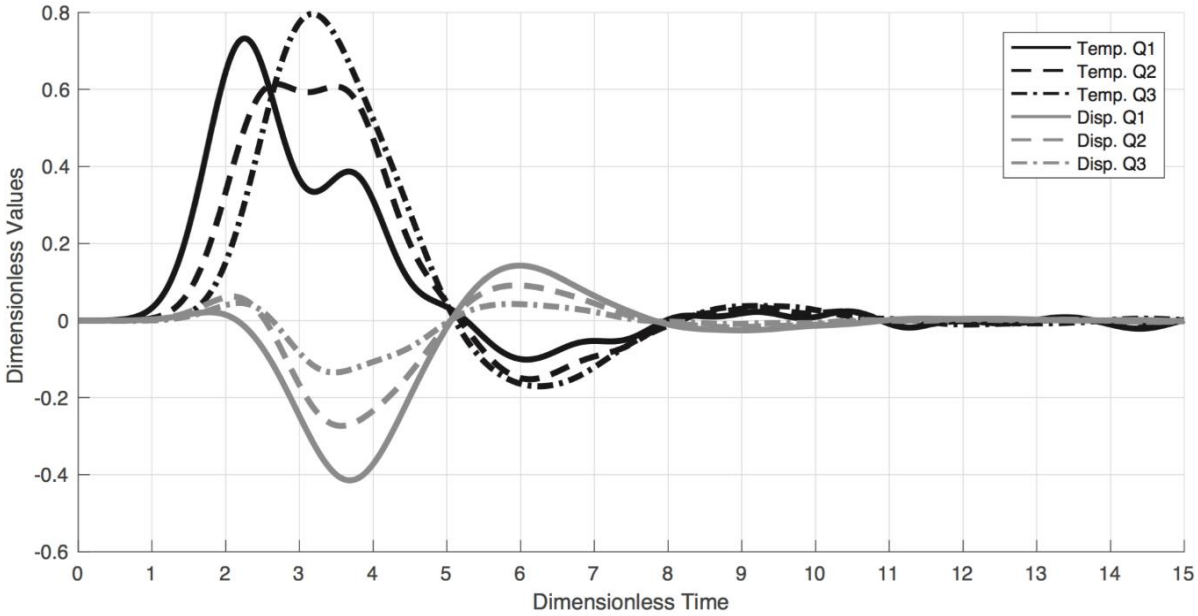

Figure 8 The propagation of thermal and elastic waves through the thickness of hollow sphere which are observed at three points under the case II of thermal loading with $\boldsymbol{a} = 0.5$.

This area is equivalent to the dissipated energy of the viscous effect. Therefore, increasing of the temperature through the time is expected, which it is against the existing results in Figure (9). These facts lead us to this conclusion that a dissipative term is missed in Eq. (5).
This dissipative term, which correspond to evanescing of mechanical stored energy in form of heat, seems to be positive definite. In this way, in any conditions, either loading or unloading, the dissipated mechanical energy appeared in form of a positive heat source in heat transfer equation. In the present study, the dissipative term was not considered in the heat balance equation, which leads to this paradox.

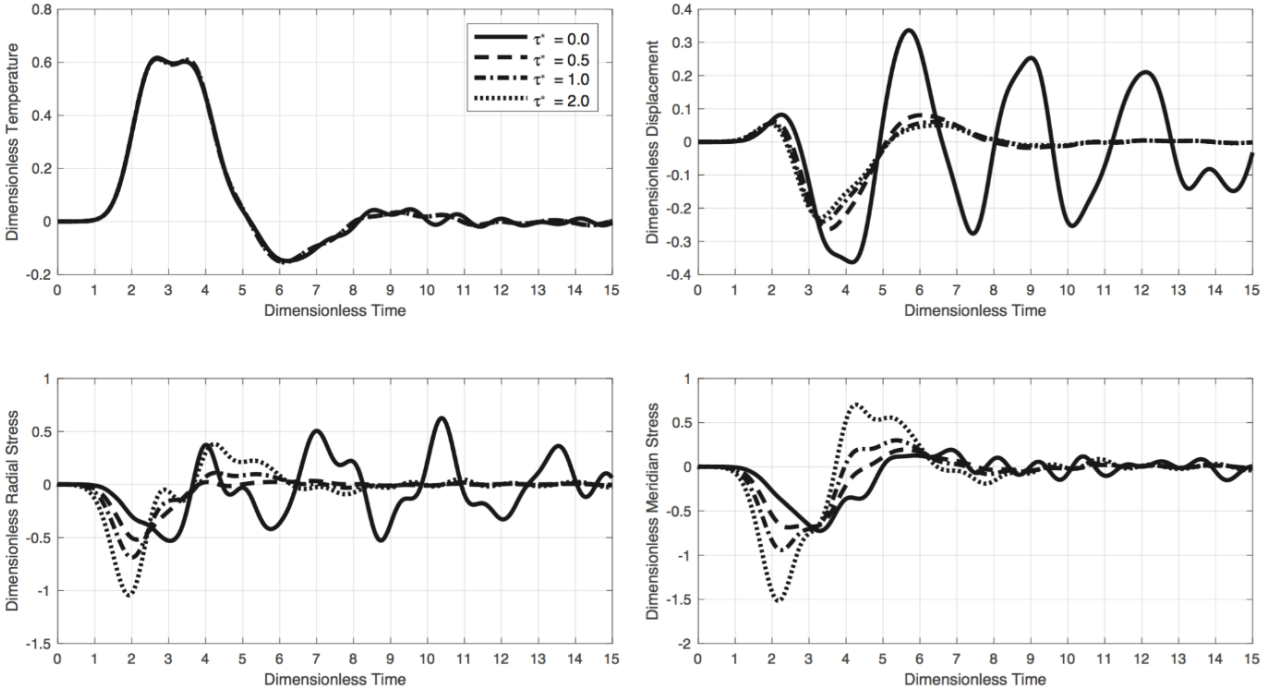

Figure 9 Variation of different dimensionless field variables with change of viscous relaxation time under the case II of thermal loading with $\boldsymbol{a} = 0.5$.

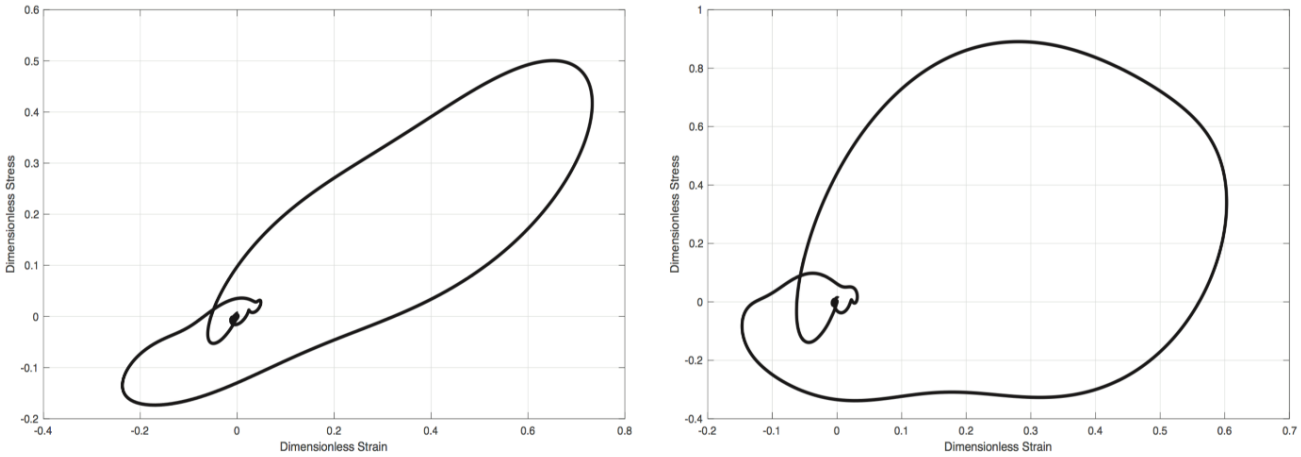

Figure 10 The stress-strain hysteresis loops caused by viscous effect under the case II of thermal loading with $\boldsymbol{a} = 0.5$, (a) $\boldsymbol{\tau}^* = 0.5$, and (b) $\boldsymbol{\tau}^* = 2.0$.

5 Conclusion

The linear generalized thermo-viscoelasticity problem of thick hollow sphere subjected to symmetrical thermal loading in the context of the theory of Lord-Shulman and the viscoelastic model of Kelvin-Voigt is obtained in this paper. Two coupled balance equations are obtained in terms of radial displacement and temperature. The resulting equations are discretized by using the Galerkin finite element method and transferred into the Laplace space to obtain a system of linear algebraic equations in Laplace space. The numerical results are achieved in time domain by using the numerical inverse Laplace method of Weeks. The numerical results are provided to show the propagation of temperature, radial displacement, radial stress, and meridian stress. Furthermore, the shortage of positive definite dissipative term in the heat balance equation is revealed. Due to this shortage, the footprints of dissipated energy by viscous effect is lost in the formulations. However, this shortcoming is repeated in many researches [14-17], continuously. Finally, it is concluded that the dissipative term is indispensable.

References

[1] Lord, H. W., and Shulman, Y., "A Generalized Dynamical Theory of Thermoelasticity", J. Mech. Phys. Solids, Vol. 15, pp. 299-309, (1967).

[2] Green, A. E., and Lindsay, K. A., "Thermoelasticity", J. Elast., Vol. 2, pp. 1-7, (1972).

[3] Green, A. E., and Naghdi, P. M., "A Re-Examination of the Basic Postulates of Thermomechanics", Proc. R. Soc. A, Vol. 432, pp. 171-194, (1991).

[4] Green, A. E., and Naghdi, P. M., "Thermoelasticity without Energy Dissipation", J. Elast., Vol. 31, pp. 189-208, (1993).

[5] Müller, I., "The Coldness, a Universal Function in Thermoelastic Bodies", Arch. Ration. Mech. Anal., Vol. 41, pp. 319-332, (1971).

[6] Green, A. E., and Laws, N., "On the Entropy Production Inequality", Arch. Ration. Mech. Anal., Vol. 45, pp. 47-53, (1972).

[7] Bagri, A., and Eslami, M. R., "A Unified Generalized Thermoelasticity; Solution for Cylinders and Spheres", Int. J. Mech. Sci., Vol. 49, pp. 1325-1335, (2007).

[8] Ignaczak, J., "A Note on Uniqueness in Thermoelasticity with One Relaxation Time", J. Therm. Stresses, Vol. 5, pp. 257-263, (1982).

[9] Chandrasekharaiah, D. S., "Thermoelasticity with Second Sound: A Review", Appl. Mech. Rev., Vol. 39, pp. 355-376, (1986).

[10] Chandrasekharaiah, D. S., "Hyperbolic Thermoelasticity: A Review of Recent Literature", Appl. Mech. Rev., Vol. 51, pp. 705-729, (1998).

[11] Bagri, A., and Eslami, M. R., "Generalized Coupled Thermoelasticity of Functionally Graded Annular Disk Considering the Lord-Shulman Theory", Compos. Struct., Vol. 83, pp. 168-179, (2008).

[12] Jabbari, M., and Dehbani, H., Exact Solution for Lord-Shulman Generalized Coupled Thermoporoelasticity in Spherical Coordinates", in R. B. Hetnarski (Editor), Encyclopedia of Thermal Stresses, Vol. 2, pp. 1412-1426, Springer, Dordrecht, (2014).

[13] Kiani, Y., and Eslami, M. R., "Generalized Thermoelasticity of Rotating Disk", Int. Mech. Aerosp. Eng., Vol. 2, pp. 23-29, (2016).

[14] Ezzat, M. A., El-Karamany, A. S., and Samaan, A. A., "State-space Formulation to Generalized Thermoviscoelasticity with Thermal Relaxation", J. Therm. Stresses, Vol. 24, pp. 823-846, (2001).

[15] Othman, M. I. A., Ezzat, M. A., Zaki, S. A., and El-Karamany, A. S., "Generalized Thermo-viscoelastic Plane Waves with Two Relaxation Times", Int. J. Eng. Sci., Vol. 40, pp. 1329-1347, (2002).

[16] El-Karamany, A. S., and Ezzat, M. A., "On the Boundary Integral Formulation of Thermo-viscoelasticity Theory" Int. J. Eng. Sci., Vol. 40, pp. 1943-1956, (2002).

[17] Kar, A., and Kanoria, M., "Generalized Thermo-visco-elastic Problem of a Spherical Shell with Three-phase-lag Effect", Appl. Math. Modell. Vol. 33, pp. 3287-3298, (2009).

[18] Weeks, W. T., "Numerical Inversion of Laplace Transforms using Laguerre Functions", J. ACM, Vol. 13, pp. 419-426, (1966).

[19] Kanoria, M., and Mallik, S. H., "Generalized Thermoviscoelastic Interaction Due to Periodically Varying Heat Source with Three-phase-lag Effect", Eur. J. Mech. A-Solid, Vol. 29, pp. 695-703, (2010).

[20] Hetnarski, R. B., and Eslami, M. R., "*Thermal Stresses, Advanced Theory and Applications*", Springer, Amsterdam, (2009).

[21] Eslami, M. R., "*Finite Elements Methods in Mechanics*", Springer, Cham, (2014).

[22] Wang, Q., and Zhan, H., "On Different Numerical Inverse Laplace Methods for Solute Transport Problems", Adv. Water Resour. Vol. 75, pp. 80-92, (2015).

[23] Eslami, M. R., and Vahedi, H., "A Galerkin Finite Element Formulation of Dynamic Thermoelasticity for Spherical Problems", Proc. 1989 ASME PVP Conf., Hawaii, (1989).

[24] Eslami, M. R., and Vahedi, H., "Galerkin Finite Element Displacement Formulation of Coupled Thermoelasticity Spherical Problems", J. Pressure Vessel Technol., Vol. 114, pp. 380-384, (1992).

Nomenclature

a	Thermal loading intensity coefficient
a_j	Weeks weight parameters
$\mathcal{B}$	Body of spherical thick sphere
c	Specific heat coefficient
c_1	Speed of propagation of primary elastic wave
C_E	Elastic coupling parameter
C_T	Thermoelastic coupling parameter
F_r	Radial force over boundary of elements
g	Weeks scaling parameter
$h(\cdot)$	Weeks weight function
$H(\cdot)$	Step function
K	Thermal conductivity coefficient
l	Characteristic length
$L_i(\cdot)$	ith Laguerre orthonormal polynomials
M	Number of Laguerre terms to approximation
n_r	Number of node per element
n_e	Number of elements
N	Shape function
q_i	components of heat flux vector
Q_r	Radial flux over boundary of elements
r	radius position
r_i, r_o	inside and outside radii
s	Laplace variable
t	time variable
t_0	Lord-Shulman relaxation time
$t_{\max}$	maximum value of time to compute with Weeks method
T	Absolute temperature
T_0	Reference temperature
T_d	Designation temperature
T_m	Nodal value of Temperature
u	radial displacement
U_m	Nodal value of displacement
$X(\cdot)$	Solution vector

Greek symbols

α	Weeks parameter
β	Thermoelastic coefficient
ε_{ij}	components of strain tensor
γ	Thermal expansion coefficient
λ, μ	Lamé coefficients
Ψ	Weeks parameter
ρ	mass density
σ	Weeks parameter
σ_{ij}	Components of stress tensor
τ	Kelvin-Voigt relaxation time
θ_i	Weeks parameters

چکیده

در این مقاله ترمو-ویسکوالاستیسیته‌ی عمومیت یافته بر روی یک کره‌ی توخالی تحت بار حرارتی متقارن بررسی شده است. برای فائق آمدن بر سرعت انتشار بی نهایت موج حرارت، مدل لرد-شلمان به کار گرفته شده است. دو معادله‌ی حرکت شعاعی و انرژی برای این کره‌ی توخالی بدست آورده شده و سپس بی‌بعد شده است. این معادلات به فضای لاپلاس برده شده و با استفاده از روش اجزای محدود گسسته شده است.
برای بدست آوردن مقادیر، روش ویکس به کار گرفته شده تا معادل آن‌ها در دامنه‌ی زمان بدست آید. در نهایت، مقادیر عددی ارائه شده تا انتشار موج حرارت و مکانیکی به نمایش درآید. این نتایج به صورت نمودارهایی در دامنه‌ی زمان و شعاع به تصویر کشیده شده‌اند.